EuroIntervention 2022;18:253-261 published online ahead of print December 2021

Near-infrared spectroscopy to predict plaque progression in plaque-free artery regions

Mariusz Tomaniak[1,2], MD; Eline M.J. Hartman[1], MD; Maria N. Tovar Forero[1], MD; Jeroen Wilschut[1], MD; Felix Zijlstra[1], MD, PhD; Nicolas M. Van Mieghem[1], MD, PhD; Isabella Kardys[1], MD, PhD; Jolanda J. Wentzel[1], PhD; Joost Daemen[1]*, MD, PhD

1. Department of Cardiology, Erasmus University Medical Center, Thorax Center, Rotterdam, the Netherlands; 2. First Department of Cardiology, Medical University of Warsaw, Warsaw, Poland

J. J. Wentzel and J. Daemen contributed equally to this manuscript.

This paper also includes supplementary data published online at: https://eurointervention.pcronline.com/doi/10.4244/EIJ-D-21-00452

KEYWORDS

- intravascular ultrasound
- optical coherence tomography
- other imaging modalities
- plaque rupture

Abstract

Background: Positive near-infrared spectroscopy (NIRS) signals might be encountered in areas without evident artery wall thickening, being typically perceived as artefacts.

Aims: We aimed to evaluate the utility of NIRS to identify artery wall regions associated with an increase in wall thickness (WT) as assessed by serial intravascular ultrasound (IVUS) and optical coherence tomography (OCT).

Methods: In this prospective, single-centre study, patients presenting with acute coronary syndrome (ACS) underwent NIRS-IVUS and OCT assessment of a non-culprit artery at baseline and 12-month follow-up. For each vessel, 1.5 mm segments were identified, matched and divided into 45 sectors. The relationship between the change in IVUS-based WT (DWT) and the presence of NIRS-positive signals and OCT-detected lipid was evaluated using linear mixed models.

Results: A total of 37 patients (38 vessels, 6,936 matched sectors) were analysed at baseline and 12 months. A total of 140/406 (34.5%) NIRS (+) sectors and 513/1,575 (32.6%) OCT-lipid (+) sectors were found to be located in thin (WT<0.5 mm) wall sectors. In the thin wall sectors, an increase in WT was significantly more pronounced in NIRS (+) vs NIRS (−) sectors (0.11 mm vs 0.06 mm, p<0.001). In the thick wall sectors, there was a decrease in WT observed that was less pronounced in the NIRS (+) versus NIRS (−) sectors (–0.08 mm vs −0.09 mm, p<0.001). Thin wall NIRS (+) OCT-lipid (+) sectors showed significant wall thickening (DWT=0.13 mm).

Conclusions: NIRS-positive signals in otherwise non-diseased arterial walls as assessed by IVUS could identify vessel wall regions prone to WT increase over 12-month follow-up. Our observations suggest that NIRS-positive signals in areas without evident wall thickening by IVUS should no longer be viewed as benign or imaging artefact.

** Corresponding author: Department of Cardiology, Room Rg-628, Erasmus University Medical Center, P.O. Box 2040, 3000 CA Rotterdam, the Netherlands. E-mail: j.daemen@erasmusmc.nl*

SUBMITTED ON 14/05/202 - REVISION RECEIVED ON 1st 08/08/2021 / 2nd 01/10/2021 - ACCEPTED ON 28/10/2021

DOI: 10.4244/EIJ-D-21-00452

Abbreviations

ACS	acute coronary syndrome
EEM	external elastic membrane
IVUS	intravascular ultrasound
LRP	lipid-rich plaque
NIRS	near-infrared spectroscopy
OCT	optical coherence tomography
PA	plaque area
PCI	percutaneous coronary intervention
WT	wall thickness

Introduction

Intravascular ultrasound (IVUS) has emerged as the "gold standard" modality for assessing the evolution of coronary atherosclerosis[1-8]. Due to its penetration depth, IVUS allows for exact quantification of plaque volume and wall thickness (WT). Whereas greyscale IVUS is less sensitive in detecting plaque-specific predictors of progression such as lipids, the combined near-infrared spectroscopy (NIRS)-IVUS catheter allows for accurate detection of lipid content with exact co-localisation of volumetric assessment by IVUS. The added clinical value of NIRS was shown by several clinical studies linking lipid-rich plaque (LRP) to future cardiovascular events[9-11].

To date, little is known on the association between LRP as detected by NIRS, baseline WT and change in WT over time. The latter is of particular importance since NIRS-positive signals might be routinely recognised in areas without evident vessel wall thickening on IVUS. Such findings are considered benign or perceived as artefacts. However, pathophysiological work has indicated lipid influx as one of the earliest stages of atherosclerosis[12]. While the histopathology of the autopsied hearts revealed that non-fibroatheromas with NIRS-positive signals (vs non-fibroatheromas without NIRS-positive signals) were mostly pathological intimal thickening (50%), with a greater prevalence of histological lipid pool or calcified nodule[13], the implications of positive NIRS signals, detected in otherwise non-diseased arteries as assessed by IVUS, have never been investigated in a prospective intravascular imaging study. Our aim was to assess the change in WT in regions with NIRS-positive and NIRS-negative signals, with and without underlying plaque as detected by IVUS, using optical coherence tomography (OCT) to confirm the actual lipid presence within the artery wall. We did so in a dedicated longitudinal follow-up study, with multimodality imaging of non-culprit arteries of patients presenting with acute coronary syndrome (ACS), and serial (baseline and 12-month) invasive imaging using NIRS-IVUS and OCT.

Editorial, see page 190

Methods

In this prospective, single-centre study, patients presenting with ACS successfully treated with percutaneous coronary intervention (PCI) underwent combined NIRS-IVUS and OCT assessment of a non-culprit coronary artery at baseline and at 12-month follow-up. All patients received guideline-recommended secondary prevention, including dual antiplatelet and lipid-lowering therapy[14]. Major exclusion criteria included: previous coronary artery bypass grafting, three-vessel disease, estimated glomerular filtration rate <50 ml/min, left ventricular ejection fraction <30% and atrial fibrillation. All patients provided written informed consent prior to enrolment. The study protocol was approved by the local ethics committee (MEC 2015-535, NL54519.078.15) and is registered (ISCRTN:43170100). The study was conducted in accordance with the Declaration of Helsinki (64th WMA general Assembly, Fortaleza, Brazil, October 2013) and the Medical Research Involving Human Subject Act (WMO).

NIRS-IVUS AND OCT ACQUISITION

A near-infrared intravascular ultrasound (NIRS-IVUS) pullback (TVC Insight Coronary Imaging Catheter; InfraRedX) (0.5 mm/s) and a 75 mm OCT acquisition (Dragonfly Optis Imaging Catheter; St. Jude Medical) (36 mm/s) were performed in the same non-stented non-culprit coronary segment with a minimum length of 30 mm and two readily identifiable side branches (diameter >1.5 mm). The study segment for invasive imaging was selected by the operator, based on the availability of optimal identifiable landmarks required for the matching of multimodality imaging data, the anticipated segment length and the feasibility of invasive local Doppler flow measurements in this cohort[15].

IVUS ANALYSIS

First, IVUS-pullbacks were ECG-gated by selecting the frame recorded six frames before the R-peak, using in-house developed software (MATLAB V.2017B; Mathworks Inc.)[16]. As a result, changes in lumen size related to the movement of the catheter or pressure changes during the contraction of the heart were removed. The gated pullback had approximately one frame every 0.5 mm. Second, image analysis of the ECG-triggered IVUS pullbacks was performed using QCU-CMS software (Version 4.69; Division of Image Processing, Leiden University Medical Center); the external elastic membrane (EEM) and lumen borders were delineated semi-automatically. Vessel WT was determined as the distance between lumen and EEM contours. An intraobserver analysis was performed in a random sample of five IVUS pullbacks (748 frames) with at least two months interval between the initial and the repeated IVUS analysis. A good reproducibility of EEM area, lumen area, and plaque area (PA) was found with an interclass correlation coefficient of 0.996 (95% CI: 0.996-0.997), 0.983 (95% CI: 0.963-0.990), and 0.958 (95% CI: 0.939-0.970), respectively. Since WT cannot be reliably quantified in regions with extensive calcification by IVUS[1], sectors with calcifications >90° of the vessel circumference were excluded[17]. Likewise, sectors were excluded in case EEM was not reliably visualised by IVUS due to any other reasons (e.g., attenuation).

Subsequently, all IVUS-analysed wall sectors were stratified into thin ("plaque-free" WT<0.5 mm) or thick ("plaque-containing" WT ≥0.5 mm) wall sectors using the previously described WT cut-off value of 0.5 mm[18].

OCT ANALYSIS

OCT pullbacks were analysed every millimetre (1 out of every 5 frames) using the QCU-CMS software following the previously published OCT analysis consensus standards[19,20]. Lumen contours were delineated semi-automatically. Lipid-rich plaque or lipid-pool were identified manually by indicating the angles with the protractor on the lumen centre **(Supplementary Appendix 1)**.

NIRS-IVUS AND OCT MATCHING AND SECTOR-LEVEL ANALYSES

Baseline OCT data and segmented IVUS follow-up data were matched to the NIRS-IVUS baseline pullback, based on side branches visible in both modalities, both in longitudinal and axial direction. All matched pullbacks were divided into paired 1.5 mm segments and further divided into eight circumferential 45° sectors **(Central illustration)**. This division was selected to ensure maximal overlap of the baseline and follow-up IVUS data, thereby allowing a maximally detailed analysis of spatial heterogeneity of WT changes. Additionally in this study, in contrast to a cross-sectional plaque burden analysis used as a measure for disease burden (plaque area/vessel area×100), a relative PA (sectorial plaque area/sectorial vessel area sector×100%) was calculated[15].

For each degree in circumference, the presence of NIRS-positive signals (a probability of 0.6 or higher for the presence of lipids), and the presence of OCT-detected lipid was determined. The sector was considered NIRS-positive or OCT-detected lipid positive in cases where the lipid content exceeded 50% of the sector area. Sectorial WT progression over the 12-month follow-up was defined as the difference between the 12-month and baseline WT **(Central illustration**, **Supplementary Figure 1**, **Supplementary Figure 2**).

STATISTICAL ANALYSIS

Continuous variables with normal distribution are presented as mean±standard deviation (SD), data with non-normal distribution are presented as median (25th-75th percentile). Categorical variables

EuroIntervention

CENTRAL ILLUSTRATION Methodology of sectorial wall thickness quantification.

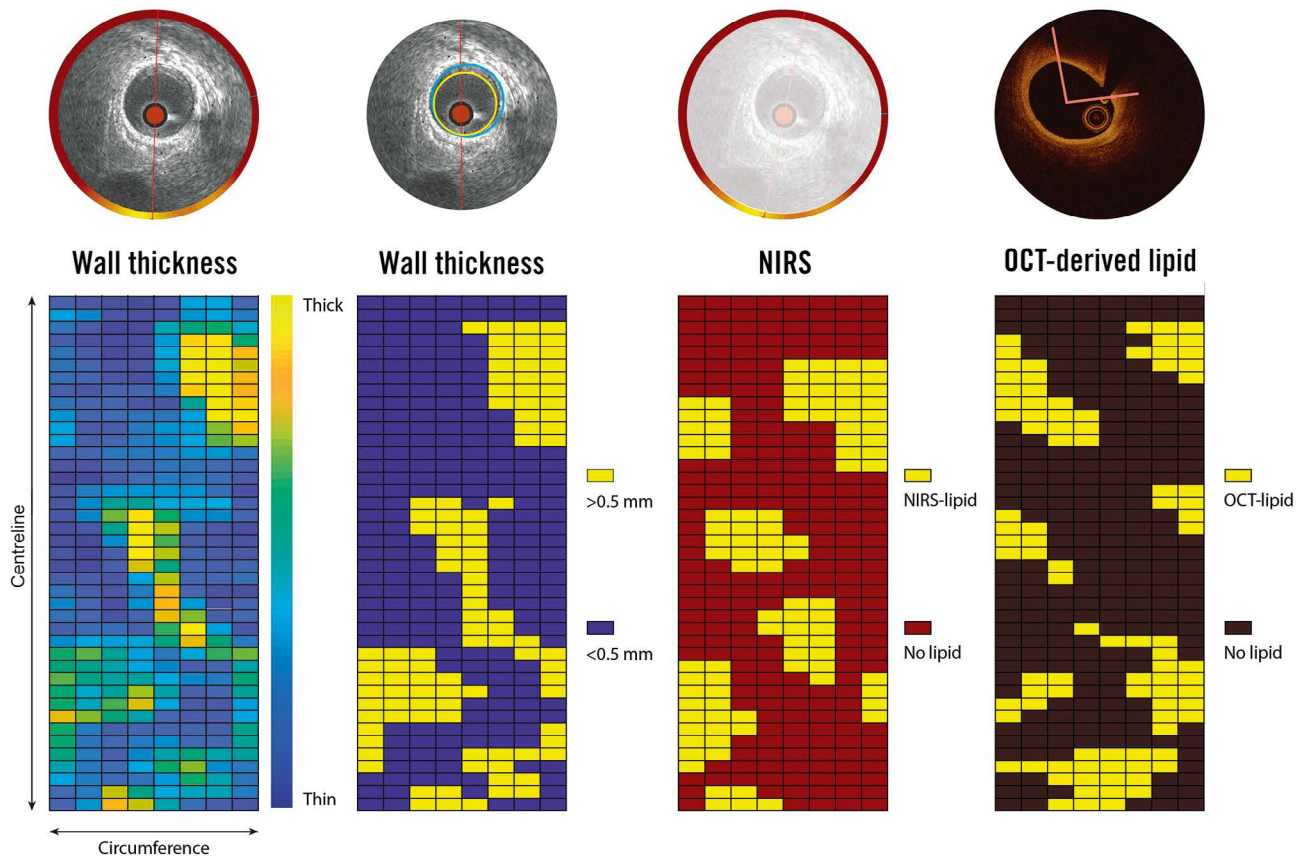

A division into paired 1.5 mm segments of 45° sectors has been selected to ensure maximal overlap of the baseline and follow-up IVUS data, even in the presence of small registration errors (max ±1 IVUS frame), thereby maximally accounting for spatial heterogeneity in WT changes. NIRS: near-infrared spectroscopy; IVUS: intravascular ultrasound; OCT: optical coherence tomography; WT: wall thickness

are displayed as counts and percentages. Differences in frequency distributions were evaluated using χ^2 tests. The association between the presence of lipid (by either NIRS or OCT) (independent variable) and the change in WT or sectorial PA (dependent variable) was analysed using linear mixed models. The presence of lipid was included as a fixed factor. To investigate the difference between plaque and plaque-free wall, the variable baseline WT was dichotomised (thin versus thick) and used as a fixed factor. Random effects were included to account for the presence of multiple sectors in each vessel. Moreover, an unstructured covariance and correlation matrix was used for the random effects to account for the covariances and correlations of the sectors. In figures presenting the association between the baseline NIRS signal or OCT-detected lipid and the change in WT (ΔWT), the estimated means and confidence intervals derived from these linear mixed models are presented. The Bonferroni correction was applied to adjust for multiple testing (repeating the analysis in above-described subgroups). Specifically, analyses were performed in the overall sectors as well as in the thin and thick wall sectors, as assessed by IVUS at baseline.

Statistical analyses were performed using the IBM SPSS Statistics 27.0 software. A two-sided p-value of <0.05 was considered as significant.

Results

Between March 2016 and March 2018, a total of 116 patients were screened based on preprocedural entry criteria and subsequently signed informed consent. Of them, 60 patients were excluded due to three-vessel disease or no anatomical landmarks in the non-stented/non-culprit vessel. Subsequently, a total of 56 patients with ACS were included in the study and underwent NIRS-IVUS and OCT assessment of a non-culprit coronary artery after successful treatment of the culprit lesion at baseline.

Three patients were excluded during the baseline procedure, four patients withdrew consent at the one-month follow-up, and eight patients refused consent for the one-year invasive imaging procedure. In one patient there was no possibility of matching between computed tomography and invasive imaging data. As a result, after successful treatment of the culprit lesion, a total of 40 patients with ACS underwent NIRS-IVUS and OCT assessment of a non-culprit coronary artery both at baseline and at 12-month follow-up. After excluding one patient due to insufficient quality NIRS data and two patients due to non-analysable OCT recordings, a total of 37 patients with 38 vessels were analysed at baseline and 12 months. Mean age was 60±8.9 years, 34 patients (91.7%) were male, 8 had diabetes (21.6%), and 16 (43.2%) presented with dyslipidaemia. The median low-density lipoprotein (LDL) level at time of enrolment was 2.8 (2.1-3.2) mmol/l. At baseline, 20 patients (54.1%) were on statin treatment (5 patients [13.5%] were on high-intensity lipid-lowering treatment) while at follow-up 33 patients (89.2%) were using lipid-lowering therapy (17 patients [45.9%] were on high-intensity lipid-lowering treatment). The baseline characteristics of the analysed population are detailed in **Table 1**.

Table 1. Baseline characteristics.

Clinical characteristics	N=37 patients
Age, years	60±8.9
Men, n (%)	34 (91.9%)
Body mass index	27±5.0
Diabetes mellitus, n (%)	8 (21.6%)
Hypertension, n (%)	9 (24.3%)
Dyslipidaemia, n (%)	16 (43.2%)
Current smoking, n (%)	9 (24.3%)
Positive family history, n (%)	13 (35.1%)
Previous MI, n (%)	8 (21.6%)
Previous PCI, n (%)	11 (29.7%)
LDL (mmol/L)	2.8 (2.1-3.2)
Statin therapy	20 (54.1%)
High-intensity lipid-lowering*	5 (13.5%)
Imaged study vessel characteristics	**N=38 vessels**
LAD, n (%)	13 (34%)
LCX, n (%)	10 (26%)
RCA, n (%)	15 (39%)
Imaged segment length, mm	50.3 (36.4-58.5)
Mean lumen area, mm^2	8.8 (7.1-11.0)
Minimum lumen area, mm^2	3.9 (2.77-5.05)
Mean vessel area, mm^2	14.9 (11.8-16.4)
Percent atheroma volume, (%)	36.5 (31.3-45.1)
Max $LCBI_{4mm}$	275.3 (166.7-392.7)

*high-intensity lipid-lowering therapy: rosuvastatin ≥20 mg or atorvastatin ≥40 mg or PCSK9-inhibitor. Data are presented as count and percentage or median and interquartile range. LAD: left anterior descending artery; LCBI: lipid core burden index; LCX: left circumflex artery; LDL: low-density lipoprotein cholesterol; MI: myocardial infarction; PCI: percutaneous coronary intervention; RCA: right coronary artery

Table 2. Imaged artery wall sectors characteristics.

Matched artery wall sectors	N=6,936	
	Baseline	12 months
Wall thickness, mm		
Thin wall NIRS (–)	0.24±0.12	0.29±0.16
Thin wall NIRS (+)	0.30±0.12	0.39±0.16
Thick wall NIRS (–)	0.74±0.22	0.66±0.23
Thick wall NIRS (+)	0.88±0.26	0.77±0.26
Relative plaque area per sector, %		
Thin wall NIRS (–)	21.6±10.0	26.4±12.9
Thin wall NIRS (+)	28.2±10.1	33.5±10.8
Thick wall NIRS (–)	51.9±9.5	48.9±11.7
Thick wall NIRS (+)	58.9±10.8	54.1±12.9
NIRS signal fraction per sector, % *		
Thin wall NIRS (–)	1.2±0.6	1.6±0.9
Thin wall NIRS (+)	80.5±17.3	27.0±37.7
Thick wall NIRS (–)	2.8±0.9	7.3±2.1
Thick wall NIRS (–)	83.4±16.9	47.3±40.4

Mean±standard deviation is presented. *Max $LCBI_{4mm}$ was 275.3 (179.7-369.5) at baseline and 238.0 (159.8-369.7) at 12-month follow-up. NIRS: near-infrared spectroscopy

The median length of the analysed segment was 50.3 mm (36.4-58.5). After excluding sectors containing side branches or extensive (>90°) calcifications **(Supplementary Table 1)**, 6,936 corresponding sectors were analysed at baseline and 12 months **(Table 2)**. At baseline, calcifications (calcifications with the angle of <90°) were found in 123 (30.3%) out of 406 NIRS-positive sectors, whereas at 12-month follow-up calcifications were observed in a total of 122 (30.0%) out of 406 NIRS-positive sectors. Overall, there were 4,552 thin wall and 2,384 thick wall sectors identified by IVUS at baseline. The median baseline WT was 0.42 mm (0.17-0.61). NIRS- and OCT-lipid positivity was found in 140 (3.1%) and 513 (11.3%) of the 4,552 thin wall sectors, respectively.

Conversely, a total of 140/406 (34.5%) NIRS-positive sectors and 513/1,575 (32.6%) OCT-lipid positive sectors were found by IVUS to be located in sectors without vessel wall thickening at baseline (WT <0.5 mm) **(Figure 1)**. The positive and negative predictive value of NIRS- versus OCT-detected lipid plaque is presented in the **Supplementary Table 2**.

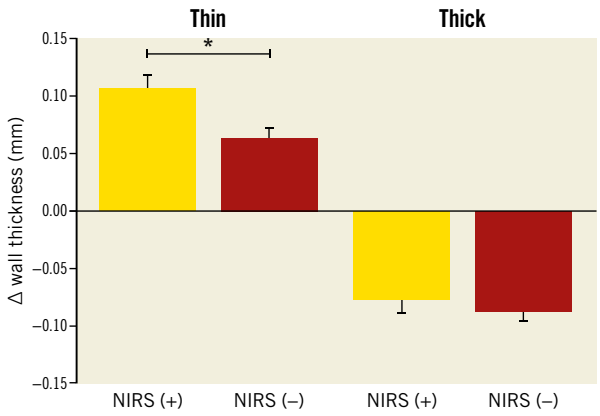

Figure 2. *Wall thickness progression in thin and thick artery wall sectors, as assessed by IVUS at baseline, stratified for the presence and absence of NIRS signal. Yellow: NIRS-positive sectors (NIRS [+]); red: NIRS-negative sectors (NIRS [−]); thin (plaque-free) <0.5 mm wall thickness by IVUS; thick ≥0.5 mm wall thickness by IVUS. *p<0.001.*

CHANGES IN WALL THICKNESS OVER 12-MONTH FOLLOW-UP

A total of 37 patients (38 vessels, 6,936 matched sectors) were analysed at baseline and 12 months. A total of 140/406 (34.5%) NIRS (+) sectors and 513/1,575 (32.6%) OCT-lipid (+) sectors were found to be located in the thin (WT<0.5 mm) wall sectors. In the thin wall sectors, an increase in WT was significantly more pronounced in NIRS (+) than in NIRS (−) sectors: 0.11 mm (95% CI: 0.08-0.13) vs 0.06 mm (95% CI: 0.05-0.08), p<0.001. In the thick wall sectors, a decrease was observed in WT that was less

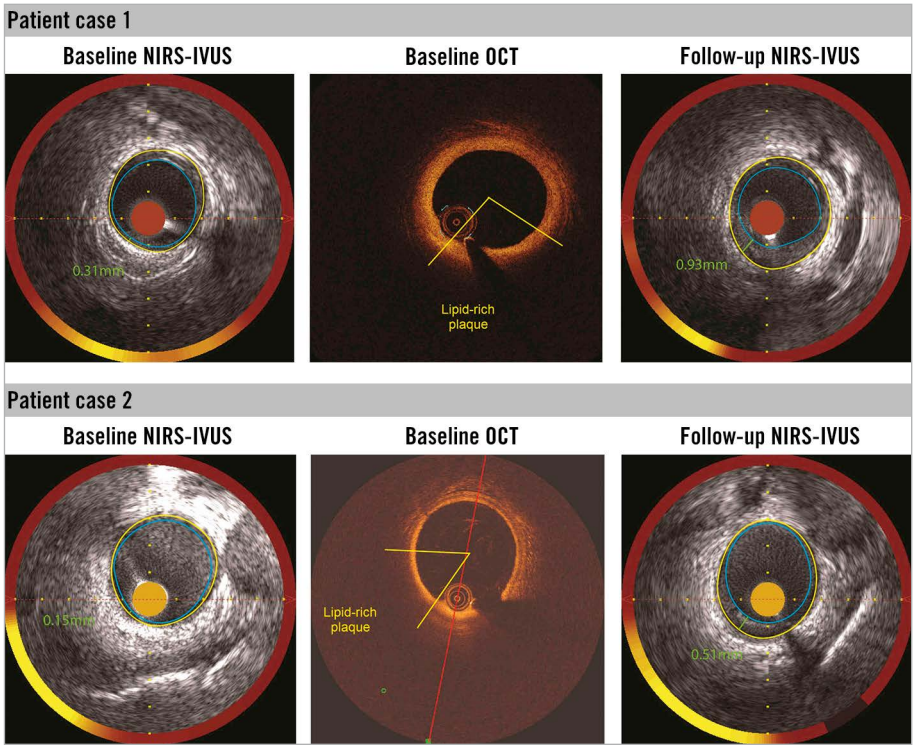

Figure 1. *Presence of NIRS signal and lipid plaque by optical coherence tomography (OCT) in the plaque free wall region (wall thickness ≤0.5 mm) as assessed by IVUS at baseline. Corresponding (matched) NIRS-IVUS and OCT cross-sections are presented. Follow-up IVUS (at 12 months) revealed artery wall thickening in the baseline NIRS-positive and OCT-lipid positive sectors. IVUS: intravascular ultrasound; NIRS: near-infrared spectroscopy*

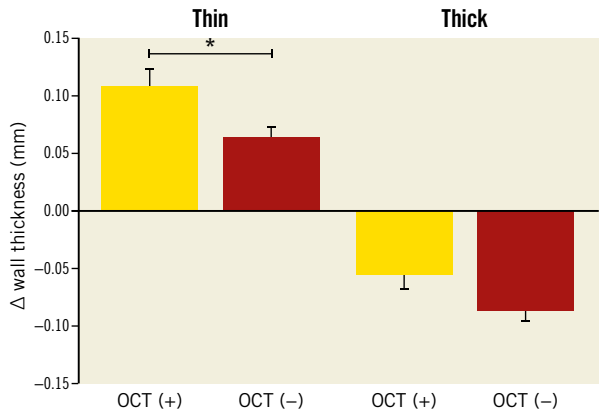

Figure 3. *Wall thickness progression in thin and thick artery wall sectors, as assessed by IVUS at baseline, stratified for the presence and absence of OCT-detected lipid plaque. Yellow: OCT-lipid plaque positive sectors (OCT [+]); red: OCT-lipid plaque negative sectors (OCT [−]); thin (plaque-free) <0.5 mm wall thickness by IVUS; thick ≥0.5 mm wall thickness by IVUS. * p<0.001.*
IVUS: intravascular ultrasound; NIRS: near-infrared spectroscopy; OCT: optical coherence tomography

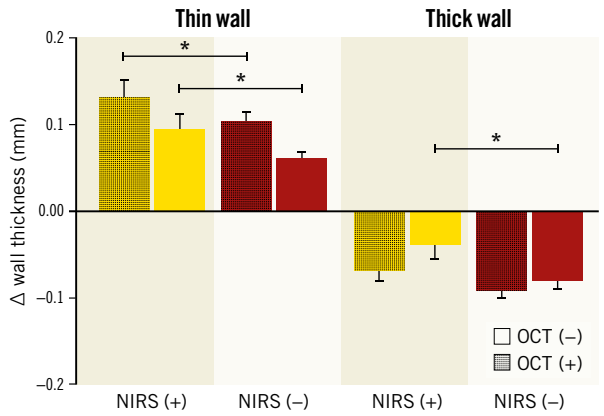

Figure 4. *Wall thickness progression in thin and thick wall sectors, stratified by NIRS- and OCT-detected lipid plaque. Yellow: NIRS-positive sectors (NIRS [+]); red: NIRS-negative sectors (NIRS [−]); thin (plaque-free) <0.5 mm wall thickness by IVUS; thick; ≥0.5 mm wall thickness by IVUS. OCT (−) sectors that did not demonstrate lipid on OCT; OCT (+): sectors that demonstrated lipid on OCT; *p<0.001. IVUS: intravascular ultrasound; NIRS: near-infrared spectroscopy; OCT: optical coherence tomography*

pronounced in NIRS (+) than in NIRS (−) sectors: −0.08 mm (95% CI: −0.10 - −0.05) vs −0.09 mm (95% CI: −0.10 - −0.07), p<0.001 **(Figure 2)**.

Similarly, the thin wall sectors with OCT-detected lipids showed significantly greater WT increase than the thin wall sectors with no OCT-detected lipids: 0.11 mm (95% CI: 0.7-0.14) vs 0.6 mm (95% CI: 0.04-0.08), p<0.001 **(Figure 3)**.

The thin wall NIRS (+) and OCT-lipid (+) sectors showed significant wall thickening (ΔWT=0.13 mm [95% CI: 0.08-0.17]) over 12 months of follow-up **(Figure 4)**. Similar patterns were observed in the changes of relative PA per sector **(Supplementary Appendix 2, Supplementary Figure 3-Supplementary Figure 5)**. Analyses adjusted for high-intensity statin use, LDL level and presence of diabetes brought consistent results **(Supplementary Table 3-Supplementary Table 6)**.

Discussion

The salient findings of this serial multimodality NIRS-IVUS and OCT imaging investigation could be summarised as follows:

1. Surprisingly, nearly one-third of all identified NIRS-positive sectors and one-third of the overall OCT-detected lipid sectors were found in thin-wall non-culprit coronary artery regions, otherwise considered as "plaque-free" sectors by IVUS, with baseline WT <0.5 mm.
2. NIRS signals imaged at baseline in thin artery wall regions were consistently associated with high WT increase at 12-month follow-up, suggesting that NIRS evaluation of non-culprit coronary arteries by IVUS could indicate the regions with ongoing plaque initiation (before any structural plaque features become detectable by IVUS).

To the best of our knowledge, this is the first in-human demonstration of the association between NIRS signals, OCT-confirmed lipid content and subsequent long-term plaque progression. Previously, Patel et al showed in diabetic and hypercholesterolaemic pigs that 88% of NIRS (+) lesions developed into a fibroatheroma over nine months of follow-up[21]. In the present study, baseline NIRS-positivity proved to be associated with more pronounced WT increase at 12 months in non-culprit segments of patients presenting with ACS. Interestingly, the observed WT increase in NIRS (+) regions was not restricted to regions with clearly visible plaque (WT >0.5 mm). Plaque growth was found to be significantly increased in NIRS (+) thin wall regions, to date typically perceived as non-diseased arteries by IVUS[1]. It therefore may be hypothesised that NIRS "chemically" captures the very early stages of plaque growth, characterised by intracellular lipid influx and accumulation[12], even before it translates into the structural changes visible by IVUS[1]. These findings above could have important clinical implications given that NIRS signals in artery regions without IVUS-defined wall thickening are typically considered as "artefact".

Considering the anticipated value of further division of the cross-sectional artery wall segments into sectors in the studies of coronary atherosclerosis[22], we have chosen to evaluate plaque progression at a sector level, analysing the sectorial changes in WT as the outcome measure in this study. By doing so, significant granularity was added to our methods which allowed us to precisely characterise the local heterogeneity in plaques growth, extending the observations from prior studies that described changes in cross-sectional plaque burden only[1-5,23,24].

The risk of major adverse cardiac events proved to increase with higher intraplaque lipid content. Patients with a maximum lipid core burden index in a 4 mm length of artery ($maxLCBI_{4mm}$) ≥400 lesion, were at a four-fold higher risk of future events as compared

to those with a maxLCBI$_{4mm}$ <400[11]. Recently, a cross-sectional *in vivo* analysis of the morphological features of NIRS-detected lipid-rich plaques showed that NIRS-positive plaques exhibit OCT and IVUS features of presumed plaque vulnerability, correlating positively with increasing lipid content[25]. Yamamoto et al previously reported that OCT-detected lipid component is a precursor for a rapid plaque progression[24]. Our work extends these observations by demonstrating that NIRS-positivity can act as a predictor of plaque growth in non-culprit coronary arteries of ACS patients, even in thin wall artery regions.

In the present study, NIRS (+) thin wall regions were apparent despite statin use at baseline in 54% of patients while the plaque growth at 12 months should be interpreted in light of the routine high-intensity statin recommendation post-ACS in all individuals; high-intensity statin therapy has been associated with plaque stabilisation or regression in previous studies. The latter might stimulate future research assessing the impact of more aggressive and costly lipid-lowering therapy including novel agents such as PCSK9 antagonists, even in case the positive NIRS signals are imaged within thin – apparently non-diseased – artery regions, as assessed by IVUS. In the present study, high-intensity statins or PCSK9 inhibitors were administered in less than half of the patients over the course of the study, indicating a potential for streamlined imaging-based uptitration of costly adjunctive lipid-lowering therapy. Nevertheless, the clinical benefits of such a therapeutic approach would need to be confirmed in a dedicated randomised trial.

Limitations

Although the presented study is the largest to date focusing on serial invasive imaging with combined use of NIRS-IVUS and OCT to study plaque progression, our findings warrant confirmation in larger studies. Despite IVUS's ability to generate high-resolution images of the entire thickness of the coronary artery wall, permitting evaluation of the entire burden of atherosclerotic plaque, it has been shown that large calcification may hinder reliable assessment of wall thickness by IVUS[1]. Given the above-mentioned considerations, artery wall regions with large calcium deposits (>90° of vessel circumference) have been excluded from the present analysis[17,26]. As a result, our study was not designed to determine the association between the presence of calcifications at baseline and plaque progression[26].

The threshold for the division of artery wall regions into 1.5 mm 45° sectors has been chosen to enhance matching accuracy. These matching/post-processing procedures were internally validated and demonstrated a high reproducibility and accuracy of sector matching; still, some minimal degree mismatch between the regions of interests analysed by the two intravascular imaging modalities, as well as the follow-up pullback, cannot be excluded.

Arguably, the lipid lowering therapy in our cohort was subpar per society guidelines that recommend high-dose statins in the context of ACS. Yet routine clinical follow-up was typically performed outside our tertiary care institution and might reflect real world practice in which more than 50% of patients treated with statins do not achieve their target LDL-C levels or cannot tolerate effective statin doses[27].

Conclusions

NIRS-positive signals and OCT-detected lipid plaque components at baseline in non-culprit coronary arteries could identify wall regions prone to WT increase over 12-month follow-up. NIRS-positive signals and OCT-derived lipid plaque might be detected in otherwise non-diseased vessel wall arteries as assessed by IVUS, having a value as predictors of early plaque growth and plaque progression in non-culprit coronary arteries. Therefore, NIRS-positive signals in areas without evident wall thickening by IVUS should no longer be viewed as benign or imaging artefact in clinical practice.

Impact on daily practice

NIRS-positive signals in otherwise non-diseased arterial walls as assessed by IVUS – typically perceived as artefacts – could identify vessel wall regions prone for wall thickness increase over 12-month follow-up. Such positive NIRS signals within the areas without evident artery wall thickening might represent a very early stage of coronary atherosclerosis and thus have a value as predictors of early plaque development in non-culprit coronary arteries. Insights from this dedicated, serial, multimodality, intravascular imaging study improve the understanding of the natural course of coronary atherosclerosis and in this context, especially early stages of atherosclerosis could help to identify potential therapeutic targets. NIRS-positive signals in areas without evident wall thickening by IVUS should no longer be viewed as benign or imaging artefact.

Funding

This work was supported by the European Research Council, Brussels, Belgium (grant number 310457).

Conflict of interest statement

M. Tomaniak acknowledges funding as the laureate of the European Society of Cardiology Research and Training Program in the form of the ESC 2018 Grant (T-2018-19628). N. Van Mieghem received research grant support from Medtronic, Abbott Vascular, Boston Scientific, Pulse Cath BV, Abiomed and Daiichi Sankyo. J.J. Wentzel was supported by a grant from ERC (310457). J. Daemen received institutional grant/research support from Astra Zeneca, Abbott Vascular, Boston Scientific, ACIST Medical, Medtronic, Microport, Pie Medical, and ReCor Medical. The other authors have no conflicts of interest to declare.

References

1. Mintz GS, Garcia-Garcia HM, Nicholls SJ, Weissman NJ, Bruining N, Crowe T, Tardif JC, Serruys PW. Clinical expert consensus document on standards for acquisition, measurement and reporting of intravascular ultrasound regression/progression studies. *EuroIntervention.* 2011;6:1123-30.

2. Tardif JC, Grégoire J, L'Allier PL, Anderson TJ, Bertrand O, Reeves F, Title LM, Alfonso F, Schampaert E, Hassan A, McLain R, Pressler ML, Ibrahim R, Lesperance J, Blue J, Heinonen T, Rodés-Cabau J; Avasimibe, Progression of Lesions on UltraSound Investigators. Effects of the acyl coenzyme A:cholesterol acyltransferase inhibitor avasimibe on human atherosclerotic lesions. *Circulation.* 2004;110:3372-7.

3. Nissen SE, Tuzcu EM, Schoenhagen P, Brown BG, Ganz P, Vogel RA, Crowe T, Howard G, Cooper CJ, Brodie B, Grines CL, DeMaria AN; REVERSAL Investigators. Effect of intensive compared with moderate lipid-lowering therapy on progression of coronary atherosclerosis: a randomized controlled trial. *JAMA.* 2004;291:1071-80.

4. Kubo T, Maehara A, Mintz GS, Doi H, Tsujita K, Choi SY, Katoh O, Nasu K, Koenig A, Pieper M, Rogers JH, Wijns W, Böse D, Margolis MP, Moses JW, Stone GW, Leon MB. The dynamic nature of coronary artery lesion morphology assessed by serial virtual histology intravascular ultrasound tissue characterization. *J Am Coll Cardiol.* 2010;55:1590-7.

5. Nissen SE, Nicholls SJ, Sipahi I, Libby P, Raichlen JS, Ballantyne CM, Davignon J, Erbel R, Fruchart JC, Tardif JC, Schoenhagen P, Crowe T, Cain V, Wolski K, Goormastic M, Tuzcu EM; ASTEROID Investigators. Effect of very high-intensity statin therapy on regression of coronary atherosclerosis: the ASTEROID trial. *JAMA.* 2006;295:1556-65.

6. Eisen HJ, Tuzcu EM, Dorent R, Kobashigawa J, Mancini D, Valantine-von Kaeppler HA, Starling RC, Sorensen K, Hummel M, Lind JM, Abeywickrama KH, Bernhardt P; RAD B253 Study Group. Everolimus for the prevention of allograft rejection and vasculopathy in cardiac-transplant recipients. *N Engl J Med.* 2003;349:847-58.

7. Jensen LO, Thayssen P, Pedersen KE, Stender S, Haghfelt T. Regression of coronary atherosclerosis by simvastatin: a serial intravascular ultrasound study. *Circulation.* 2004;110:265-70.

8. Okazaki S, Yokoyama T, Miyauchi K, Shimada K, Kurata T, Sato H, Daida H. Early statin treatment in patients with acute coronary syndrome: demonstration of the beneficial effect on atherosclerotic lesions by serial volumetric intravascular ultrasound analysis during half a year after coronary event: the ESTABLISH Study. *Circulation.* 2004;110:1061-8.

9. Schuurman AS, Vroegindewey M, Kardys I, Oemrawsingh RM, Cheng JM, de Boer S, Garcia-Garcia HM, van Geuns RJ, Regar ES, Daemen J, van Mieghem NM, Serruys PW, Boersma E, Akkerhuis KM. Near-infrared spectroscopy-derived lipid core burden index predicts adverse cardiovascular outcome in patients with coronary artery disease during long-term follow-up. *Eur Heart J.* 2018;39:295-302.

10. Oemrawsingh RM, Cheng JM, Garcia-Garcia HM, van Geuns RJ, de Boer SP, Simsek C, Kardys I, Lenzen MJ, van Domburg RT, Regar E, Serruys PW, Akkerhuis KM, Boersma E; ATHEROREMO-NIRS Investigators. Near-infrared spectroscopy predicts cardiovascular outcome in patients with coronary artery disease. *J Am Coll Cardiol.* 2014;64:2510-8.

11. Waksman R, Di Mario C, Torguson R, Ali ZA, Singh V, Skinner WH, Artis AK, Cate TT, Powers E, Kim C, Regar E, Wong SC, Lewis S, Wykrzykowska J, Dube S, Kazziha S, van der Ent M, Shah P, Craig PE, Zou Q, Kolm P, Brewer HB, Garcia-Garcia HM; LRP Investigators. Identification of patients and plaques vulnerable to future coronary events with near-infrared spectroscopy intravascular ultrasound imaging: a prospective, cohort study. *Lancet.* 2019;394:1629-37.

12. Libby P, Hansson GK. From Focal Lipid Storage to Systemic Inflammation: JACC Review Topic of the Week. *J Am Coll Cardiol.* 2019;74:1594-607.

13. Kang SJ, Mintz GS, Pu J, Sum ST, Madden SP, Burke AP, Xu K, Goldstein JA, Stone GW, Muller JE, Virmani R, Maehara A. Combined IVUS and NIRS detection of fibroatheromas: histopathological validation in human coronary arteries. *JACC Cardiovasc Imaging.* 2015;8:184-94.

14. Roffi M, Patrono C, Collet JP, Mueller C, Valgimigli M, Andreotti F, Bax JJ, Borger MA, Brotons C, Chew DP, Gencer B, Hasenfuss G, Kjeldsen K, Lancellotti P, Landmesser U, Mehilli J, Mukherjee D, Storey RF, Windecker S; ESC Scientific Document Group. 2015 ESC Guidelines for the management of acute coronary syndromes in patients presenting without persistent ST-segment elevation: Task Force for the Management of Acute Coronary Syndromes in Patients Presenting without Persistent ST-Segment Elevation of the European Society of Cardiology (ESC). *Eur Heart J.* 2016;37:267-315.

15. Hartman EMJ, De Nisco G, Kok AM, Hoogendoorn A, Coenen A, Mastik F, Korteland SA, Nieman K, Gijsen FJH, van der Steen AFW, Daemen J, Wentzel JJ. Lipid-rich Plaques Detected by Near-infrared Spectroscopy Are More Frequently Exposed to High Shear Stress. *J Cardiovasc Transl Res.* 2021;14:416-25.

16. Hoogendoorn A, den Hoedt S, Hartman EMJ, Krabbendam-Peters I, Te Lintel Hekkert M, van der Zee L, van Gaalen K, Witberg KT, Dorst K, Ligthart JMR, Drouet L, Van der Heiden K, van Lennep JR, van der Steen AFW, Duncker DJ, Mulder MT, Wentzel JJ. Variation in Coronary Atherosclerosis Severity Related to a Distinct LDL (Low-Density Lipoprotein) Profile: Findings From a Familial Hypercholesterolemia Pig Model. *Arterioscler Thromb Vasc Biol.* 2019;39:2338-52.

17. Mintz GS, Nissen SE, Anderson WD, Bailey SR, Erbel R, Fitzgerald PJ, Pinto FJ, Rosenfield K, Siegel RJ, Tuzcu EM, Yock PG. American College of Cardiology Clinical Expert Consensus Document on Standards for Acquisition, Measurement and Reporting of Intravascular Ultrasound Studies (IVUS). A report of the American College of Cardiology Task Force on Clinical Expert Consensus Documents. *J Am Coll Cardiol.* 2001;37:1478-92.

18. Tuzcu EM, Kapadia SR, Tutar E, Ziada KM, Hobbs RE, McCarthy PM, Young JB, Nissen SE. High prevalence of coronary atherosclerosis in asymptomatic teenagers and young adults: evidence from intravascular ultrasound. *Circulation.* 2001;103:2705-10.

19. Tearney GJ, Regar E, Akasaka T, Adriaenssens T, Barlis P, Bezerra HG, Bouma B, Bruining N, Cho JM, Chowdhary S, Costa MA, de Silva R, Dijkstra J, Di Mario C, Dudek D, Falk E, Feldman MD, Fitzgerald P, Garcia-Garcia HM, Gonzalo N, Granada JF, Guagliumi G, Holm NR, Honda Y, Ikeno F, Kawasaki M, Kochman J, Koltowski L, Kubo T, Kume T, Kyono H, Lam CC, Lamouche G, Lee DP, Leon MB, Maehara A, Manfrini O, Mintz GS, Mizuno K, Morel MA, Nadkarni S, Okura H, Otake H, Pietrasik A, Prati F, Raber L, Radu MD, Rieber J, Riga M, Rollins A, Rosenberg M, Sirbu V, Serruys PW, Shimada K, Shinke T, Shite J, Siegel E, Sonoda S, Suter M, Takarada S, Tanaka A, Terashima M, Thim T, Uemura S, Ughi GJ, van Beusekom HM, van der Steen AF, van Es GA, van Soest G, Virmani R, Waxman S, Weissman NJ, Weisz G; International Working Group for Intravascular Optical Coherence Tomography (IWG-IVOCT). Consensus standards for acquisition, measurement, and reporting of intravascular optical coherence tomography studies: a report from the International Working Group for Intravascular Optical Coherence Tomography Standardization and Validation. *J Am Coll Cardiol.* 2012;59:1058-72.

20. Johnson TW, Räber L, di Mario C, Bourantas C, Jia H, Mattesini A, Gonzalo N, de la Torre Hernandez JM, Prati F, Koskinas K, Joner M, Radu MD, Erlinge D, Regar E, Kunadian V, Maehara A, Byrne RA, Capodanno D, Akasaka T, Wijns W, Mintz GS, Guagliumi G. Clinical use of intracoronary imaging. Part 2: acute coronary syndromes, ambiguous coronary angiography findings, and guiding interventional decision-making: an expert consensus document of the European Association of Percutaneous Cardiovascular Interventions. *Eur Heart J.* 2019;40:2566-84.

21. Patel D, Hamamdzic D, Llano R, Patel D, Cheng L, Fenning RS, Bannan K, Wilensky RL. Subsequent development of fibroatheromas with inflamed fibrous caps can be predicted by intracoronary near infrared spectroscopy. *Arterioscler Thromb Vasc Biol.* 2013;33:347-53.

22. Timmins LH, Molony DS, Eshtehardi P, McDaniel MC, Oshinski JN, Samady H, Giddens DP. Focal association between wall shear stress and clinical coronary artery disease progression. *Ann Biomed Eng.* 2015;43:94-106.

23. Nissen SE, Tuzcu EM, Libby P, Thompson PD, Ghali M, Garza D, Berman L, Shi H, Buebendorf E, Topol EJ; CAMELOT Investigators. Effect of antihypertensive agents on cardiovascular events in patients with coronary disease and normal blood pressure: the CAMELOT study: a randomized controlled trial. *JAMA.* 2004;292:2217-25.

24. Yamamoto MH, Yamashita K, Matsumura M, Fujino A, Ishida M, Ebara S, Okabe T, Saito S, Hoshimoto K, Amemiya K, Yakushiji T, Isomura N, Araki H, Obara C, McAndrew T, Ochiai M, Mintz GS, Maehara A. Serial 3-Vessel Optical Coherence Tomography and Intravascular Ultrasound Analysis of Changing Morphologies Associated With Lesion Progression in Patients With Stable Angina Pectoris. *Circ Cardiovasc Imaging.* 2017;10:e006347.

25. Zanchin C, Ueki Y, Losdat S, Fahrni G, Daemen J, Ondracek AS, Häner JD, Stortecky S, Otsuka T, Siontis GCM, Rigamonti F, Radu M, Spirk D, Kaiser C, Engstrom T, Lang I, Koskinas KC, Räber L. In vivo relationship between near-infrared spectroscopy-detected lipid-rich plaques and morphological plaque characteristics by optical coherence tomography and intravascular ultrasound: a multimodality intravascular imaging study. *Eur Heart J Cardiovasc Imaging.* 2020;22:824-34.

26. Hartman EMJ, Hoogendoorn A, Akyildiz AC, Schuurman AS, van der Steen AFW, Boersma E, Wentzel JJ, Daemen J. Colocalization of Intracoronary Lipid-Rich Plaques and Calcifications: An Integrated NIRS-IVUS Analysis. *JACC Cardiovasc Imaging.* 2020;13:1627-8.

27. Koskinas KC, Gencer B, Nanchen D, Branca M, Carballo D, Klingenberg R, Blum MR, Carballo S, Muller O, Matter CM, Lüscher TF, Rodondi N, Heg D, Wilhelm M, Räber L, Mach F, Windecker S. Eligibility for PCSK9 inhibitors based on the 2019 ESC/EAS and 2018 ACC/AHA guidelines. *Eur J Prev Cardiol.* 2021;28:59-65.

Supplementary data

Supplementary Appendix 1. Methods.

Supplementary Appendix 2. Results.

Supplementary Table 1. Reasons for sector exclusions.

Supplementary Table 2. Positive and negative predictive value of NIRS-positive signals vs OCT-detected lipid plaque.

Supplementary Table 3. Changes in wall thickness (WT) in thin and thick artery regions over 12-month follow-up, categorised according to NIRS-detected lipid-rich plaque. Analysis adjusted for high-intensity statin use, LDL level and presence of diabetes.

Supplementary Table 4. Changes in wall thickness (WT) in thin and thick artery regions over 12-month follow-up, categorised according to NIRS- and OCT-detected lipid at baseline. Analysis adjusted for high-intensity statin use, LDL level and presence of diabetes.

Supplementary Table 5. Changes in relative plaque area (per sector) in thin and thick artery regions over 12-month follow-up, categorised according to NIRS-detected lipid-rich plaque. Analysis adjusted for high-intensity statin use, LDL level and presence of diabetes.

Supplementary Table 6. Changes in relative plaque area (per sector) in thin and thick artery regions over 12-month follow-up, categorised according to NIRS- and OCT-detected lipid at baseline. Analysis adjusted for high-intensity statin use, LDL level and presence of diabetes.

Supplementary Figure 1. Overlay of luminal area of IVUS and OCT.

Supplementary Figure 2. 2D maps of wall thickness IVUS baseline and follow-up, visual check on WT patterns.

Supplementary Figure 3. Relative plaque area (per sector) progression in thin and thick artery wall sectors as assessed by IVUS at baseline stratified for the presence and absence of NIRS signals.

Supplementary Figure 4. Relative plaque area (per sector) progression in thin and thick artery wall sectors as assessed by IVUS at baseline stratified for the presence and absence of OCT-detected lipid plaque.

Supplementary Figure 5. Relative plaque area (per sector) progression in thin and thick wall sectors stratified by NIRS- and OCT-detected lipid plaque.

The supplementary data are published online at: https://eurointervention.pcronline.com/doi/10.4244/EIJ-D-21-00452

Supplementary data

Supplementary Appendix 1. Methods

Matching procedures

Multiple validation steps were used during the matching process of IVUS and OCT both baseline and at follow-up. Both OCT and IVUS follow-up were matched with baseline IVUS. Matching was performed with all side branches visible in the two imaging modalities, both in longitudinal and circumferential direction. Visible large calcifications were used as control landmarks after matching.

Based on all matched imaging modalities, a luminal area correlation was performed **(Supplementary Figure 1)**.

Rotational matching was checked by creating 2D maps by cutting open the vessel in longitudinal direction of the matched wall thickness and plaque components (IVUS-IVUS: Wall thickness patterns & calcifications, IVUS-OCT: calcifications **(Supplementary Figure 2).**

Subsequently, by fusing the 3D spatial information on the coronary vessel centreline segmented from the CCTA and the lumen contours extracted from the IVUS, a 3D reconstruction was made in MeVisLab (MeVis Medical Solutions AG). The data from the two imaging modalities were matched using large side branches as landmarks, visible in both acquisitions. The regions proximal and distal to the IVUS-derived region of interest, as well as side branches (>1.5 mm) were segmented on the CCTA and scaled and fused with the 3D reconstruction [7]. Of note, for final analysis, only the IVUS-derived region of interest (ROI) was considered.

By using side branches as landmarks, both the analysed OCT data, as well as the segmented IVUS follow-up contours, were matched to the IVUS baseline pullback. Matching was performed in both longitudinal and circumferential directions. The axial adjustment in the matching process has been performed using a dedicated matching software (linear rotational between the two side-branches) QCU-CMS software (Version 4.69; Division of Image Processing, Leiden University Medical Center). All matched and analysed data was mapped

and interpolated on the IVUS-based region of interest (ROI) on the 3D mesh geometry using VMTK (Orobix) and MATLAB (v2017b; Mathworks Inc.). For further analysis, the 3D-ROIs were divided into 1.5 mm segments, which were then further divided into 45 degrees sectors (**Figure 1**). All continuous data for each sector (i.e., OCT lipid plaque) was an average of the mesh data in that sector and has been presented as percentage. Lipid-rich plaque was defined as a region with an inhomogeneous, slowly attenuating signal and an invisible EEM. A lipid-pool was defined as a region with a sudden drop in signal with a diffuse border and an overlying signal rich cap structure. As there were only 124 sectors identified with a lipid pool at baseline (out of the overall 6,936 analysed sectors), the OCT lipid sectors included both the lipid-rich and the lipid pools together.

Supplementary Appendix 2. Results

Changes in plaque area over 12-month follow-up.

Overall, the thin wall artery regions showed significant increase, whereas the thick wall artery regions showed significant decrease in relative plaque area (PA) of the sector (mean Δ PA: 5.0% [95% CI: 4.0–6.7] vs -3.3% [95% CI: -4.7 – -2.0%]; p<0.001). The near-infrared spectroscopy (NIRS)-positive sectors showed significant plaque progression, whereas no significant progression was observed in the NIRS negative sectors (mean ΔPA: 2.9% [95% CI: 1.5–4.4] vs 1.0% [95% CI: -0.1–2.2]; p<0.001) **(Supplementary Figure 3)**.

Plaque progression was more pronounced in the NIRS-positive sectors within the thin wall regions and plaque regression in regions with already established plaques (thick regions) was significantly smaller in the NIRS-positive sectors. In the thin wall regions, the mean ΔPA in NIRS(+) vs NIRS(-) sectors was (7.9% [95% CI: 6.0–9.7]) vs (5.4% [95% CI: 4.2–6.6]), respectively, p<0.001. In the thick wall regions, the mean ΔPA in NIRS(+) vs NIRS(-) sectors was (-2.0% [95% CI: -3.6 – -0.4]) vs (-3.3% [95% CI: -4.5 – -2.1]), p<0.001. **(Supplementary Figure 4)**

Similarly, the thin wall sectors with OCT-detected lipids showed significantly higher plaque growth than the thin wall sectors with no OCT-detected lipids (7.9% [95% CI: 5.4–11]) vs (5.2% [95% CI: 2.7–7.7]). The thin wall NIRS positive sectors, for which the presence of lipid content was confirmed by OCT, showed significant plaque growth (9.3% [95% CI: 6.4–9.3]) (**Supplementary Figure 5**). Analyses adjusted for high-intensity statin use, LDL level and presence of diabetes brought consistent results **(Supplementary Table 5, Supplementary Table 6)**.

Supplementary Table 1. Reasons for sectors exclusions.

Overall sectors:	**9,906 sectors**
Not available OCT data due to e.g., non-analysable frames due to flushing artefacts, matching etc.	2,207 sectors
Not available NIRS data due to e.g., guidewire artefacts	212 sectors
Not available due to calcium (baseline)	391 sectors
Not available due to "artefact" (baseline)	30 sectors
Not available due to calcium (follow-up)	121 sectors
Not available due to artefact (follow-up)	9 sectors
Number of sectors included in the final analysis	**6,936 sectors**

OCT: optical coherence tomography; NIRS: near-infrared spectroscopy

Supplementary Table 2. Positive and negative predictive value of NIRS positive signal vs OCT-detected lipid plaque.

NIRS lipid-rich plaque	OCT-detected lipid plaque	
	PPV	55.9%
	NPV	96.7%

OCT: optical coherence tomography; NIRS: near-infrared spectroscopy; NPV: negative predictive value; PPV: positive predictive value

Supplementary Table 3. Changes in wall thickness (WT) in thin and thick artery regions over 12-month follow-up, categorised according to NIRS detected lipid rich plaque. Analysis adjusted for high-intensity statin use, LDL level and presence of diabetes.

Wall thickness	NIRS	Mean ΔWT (mm)	95% CI		*p*-value
			Lower bound	Upper bound	
Thin wall	NIRS (-)	0.07	0.05	0.09	p<0.001
	NIRS (+)	0.12	0.08	0.14	
Thick wall	NIRS (-)	-0.08	-0.11	-0.06	p<0.001
	NIRS (+)	-0.07	-0.10	-0.05	

ΔWT: change in wall thickness; LDL: low-density lipoproteins; NIRS: near-infrared spectroscopy

Supplementary Table 4. Changes in wall thickness (WT) in thin and thick artery regions over 12-month follow-up, categorised according to NIRS and OCT-detected lipid at baseline. Analysis adjusted for high-intensity statin use, LDL level and presence of diabetes.

Wall thickness	NIRS	OCT- Lipid	Mean ΔWT (mm)	95% confidence interval	
				Lower bound	Upper bound
Thin wall	NIRS (-)	OCT- lipid (-)	0.07	0.04	0.09
	NIRS (-)	OCT- lipid (+)	0.11	0.08	0.13
	NIRS (+)	OCT- lipid (-)	0.08	0.03	0.13
	NIRS (+)	OCT- lipid (+)	0.13	0.07	0.18
Thick wall	NIRS (-)	OCT- lipid (-)	-0.08	-0.10	-0.05
	NIRS (-)	OCT- lipid (+)	-0.09	-0.11	-0.06
	NIRS (+)	OCT- lipid (-)	-0.05	-0.10	-0.004
	NIRS (+)	OCT- lipid (+)	-0.06	-0.11	-0.02

ΔWT: change in wall thickness; LDL: low-density lipoproteins; OCT: optical coherence tomography; NIRS: near-infrared spectroscopy

Supplementary Table 5. Changes in relative plaque area (per sector) in thin and thick artery regions over 12-month follow-up, categorised according to NIRS detected lipid rich plaque. Analysis adjusted for high-intensity statin use, LDL level and presence of diabetes.

Wall thickness	NIRS	Mean ΔPA (%)	95% confidence interval		
			Lower bound	Upper bound	*p*-value
Thin wall	NIRS (-)	5.5	4.1	7.0	p<0.001
	NIRS (+)	8.0	6.0	10.0	
Thick wall	NIRS (-)	-3.2	-4.6	-1.7	p<0.001
	NIRS (+)	-1.8	-3.6	-0.1	

ΔPA: change in relative (sectorial) plaque area; NIRS: near-infrared spectroscopy

Supplementary Table 6. Changes in relative plaque area (per sector) in thin and thick artery regions over 12-month follow-up, categorised according to NIRS and OCT-detected lipid at baseline. Analysis adjusted for high-intensity statin use, LDL level and presence of diabetes.

Wall thickness	NIRS	OCT- lipid	Mean ΔPA (%)	95% confidence interval	
				Lower bound	Upper bound
Thin wall	NIRS (-)	OCT-lipid (-)	5.5	4.3	6.7
	NIRS (-)	OCT-lipid (+)	8.2	6.7	9.6
	NIRS (+)	OCT-lipid (-)	6.8	4.1	9.5
	NIRS (+)	OCT-lipid (+)	9.0	5.9	12.1
Thick wall	NIRS (-)	OCT-lipid (-)	-3.2	-0.4	-1.9
	NIRS (-)	OCT-lipid (+)	-2.8	-4.1	-1.5
	NIRS (+)	OCT-lipid (-)	-1.6	-4.3	1.0
	NIRS (+)	OCT-lipid (+)	-1.2	-3.4	-1.0

ΔPA: change in relative (sectorial) plaque area; LDL: low-density lipoproteins; NIRS: near-infrared spectroscopy

Supplementary Figure 1. Overlay of luminal area of IVUS and OCT.

X: axis frame numbers OCT (5 frames per 1 mm); Y: axis luminal area

IVUS: intravascular ultrasound; OCT: optical coherence tomography

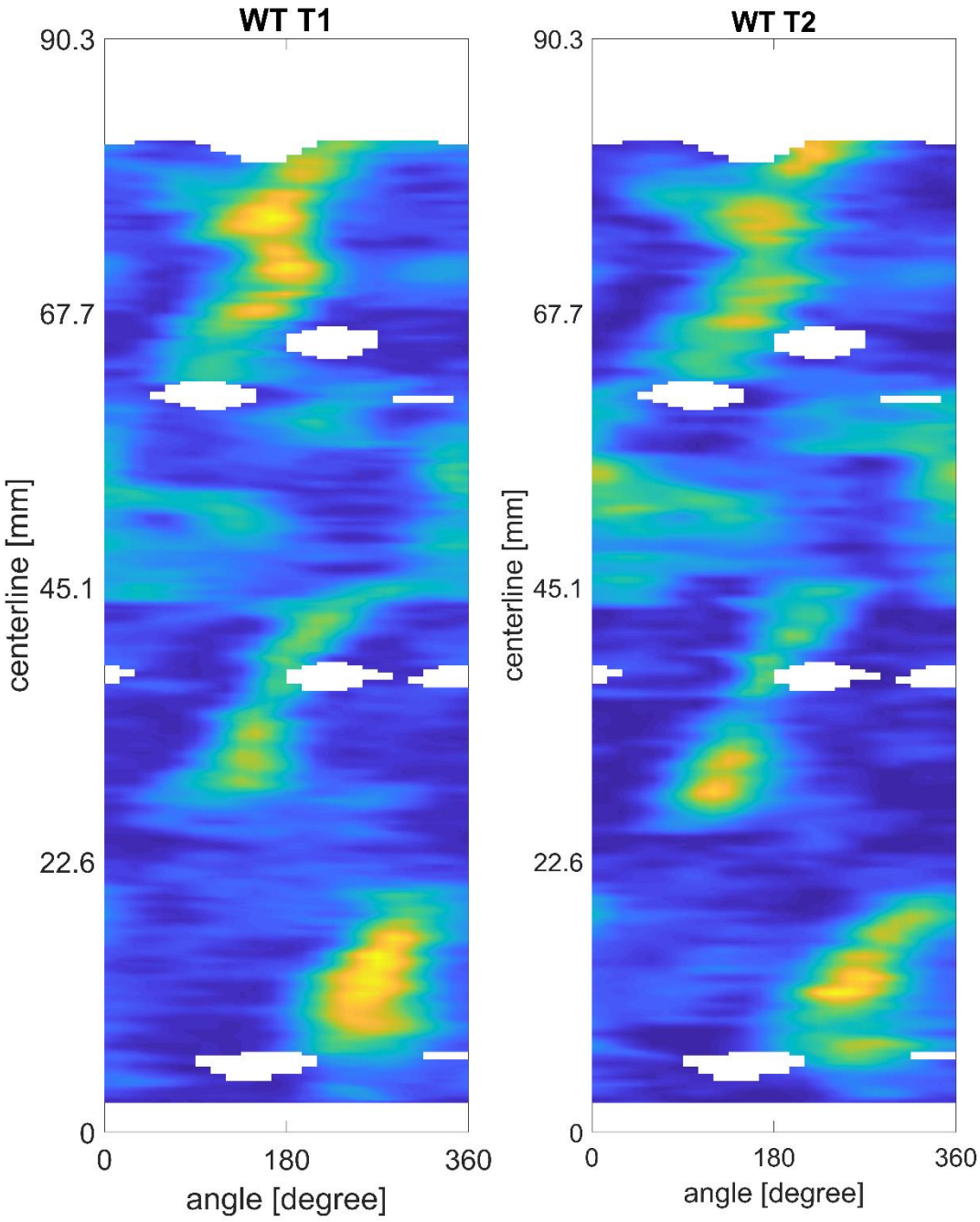

Supplementary Figure 2. 2D maps of wall thickness IVUS baseline and follow-up, visual check on WT patterns.

White regions in the 2D maps are side branches or calcifications.

IVUS: intravascular ultrasound

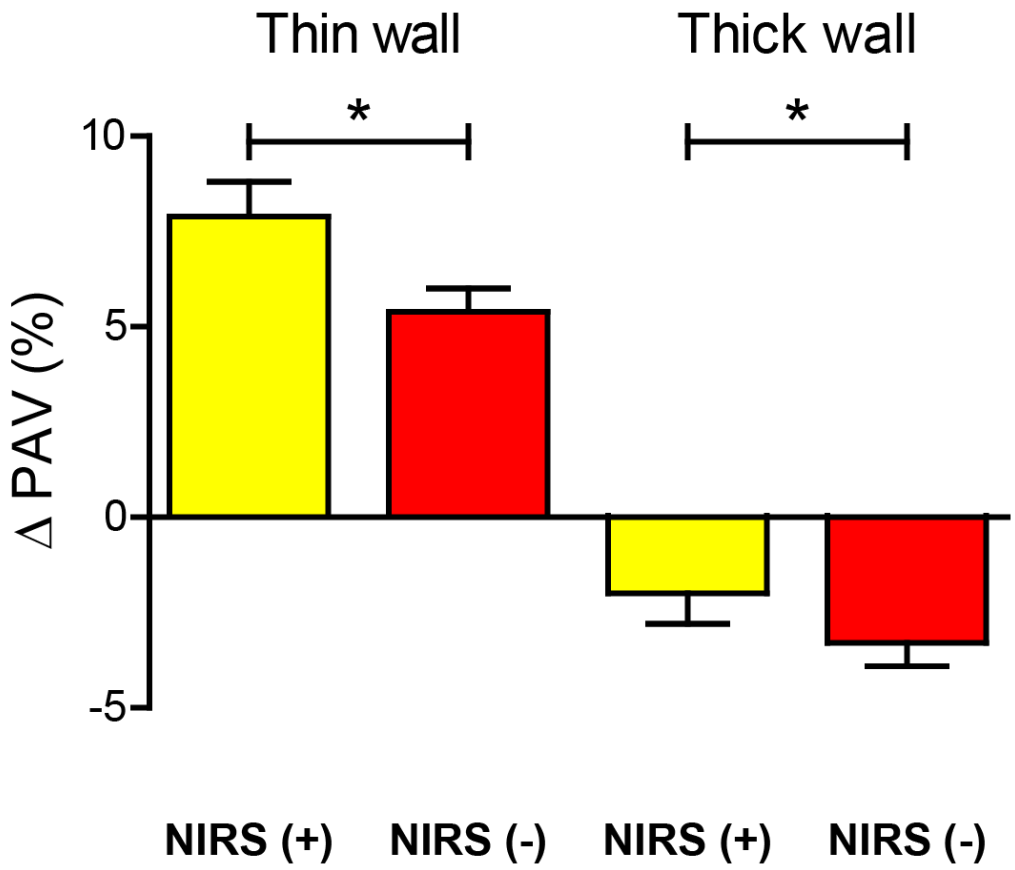

Supplementary Figure 3. Relative plaque area (per sector) progression in thin and thick artery wall sectors as assessed by IVUS at baseline stratified for the presence and absence of NIRS signal.

Yellow: NIRS positive sectors (NIRS[+]); red: NIRS negative sectors (NIRS[-]); thin <0.5 mm wall thickness by IVUS; thick ≥0.5 mm wall thickness. * p<0.001.

IVUS: intravascular ultrasound; NIRS: near-infrared spectroscopy; ΔPAV: Change in relative plaque area

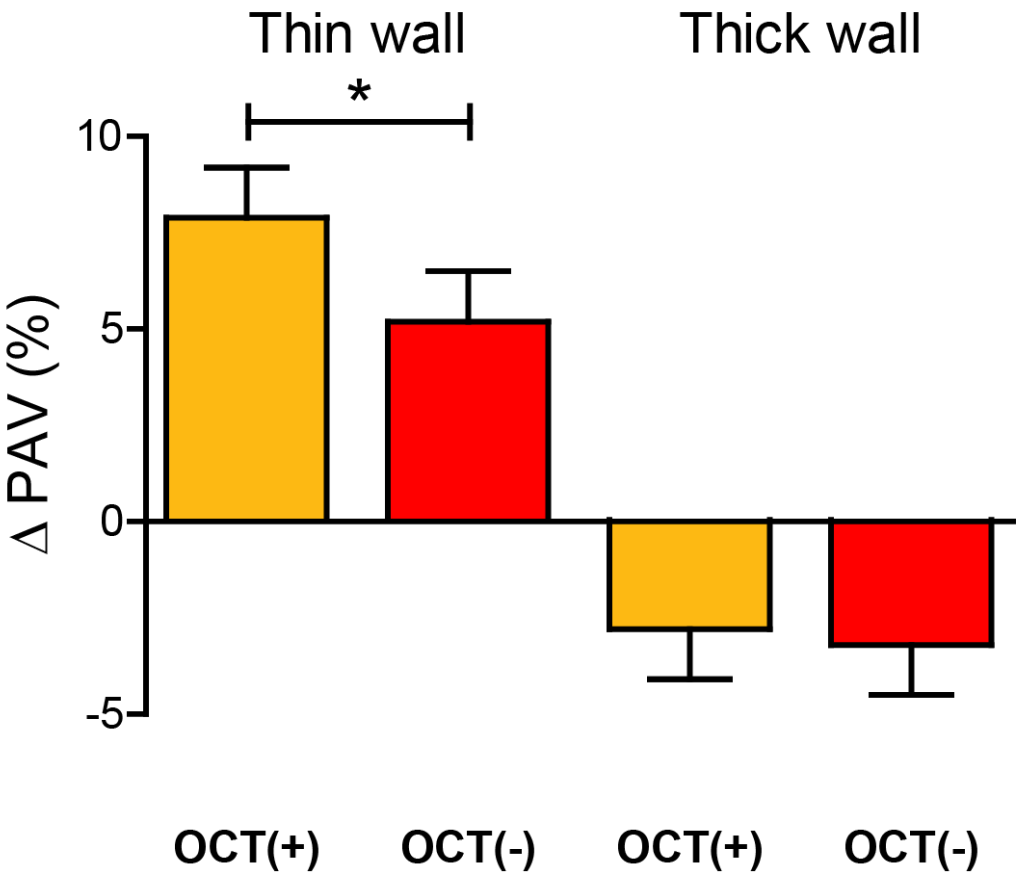

Supplementary Figure 4. Relative plaque area (per sector) progression in thin and thick artery wall sectors as assessed by IVUS at baseline stratified for the presence and absence of OCT-detected lipid plaque.

Yellow: OCT-lipid plaque positive sectors (OCT[+]); red: OCT-lipid plaque negative sectors (OCT[-]); thin <0.5 mm wall thickness by IVUS; thick ≥0.5 mm wall thickness.

* $p<0.001$

IVUS: intravascular ultrasound; OCT: optical coherence tomography; NIRS: near-infrared spectroscopy; ΔPAV: Change in relative plaque area

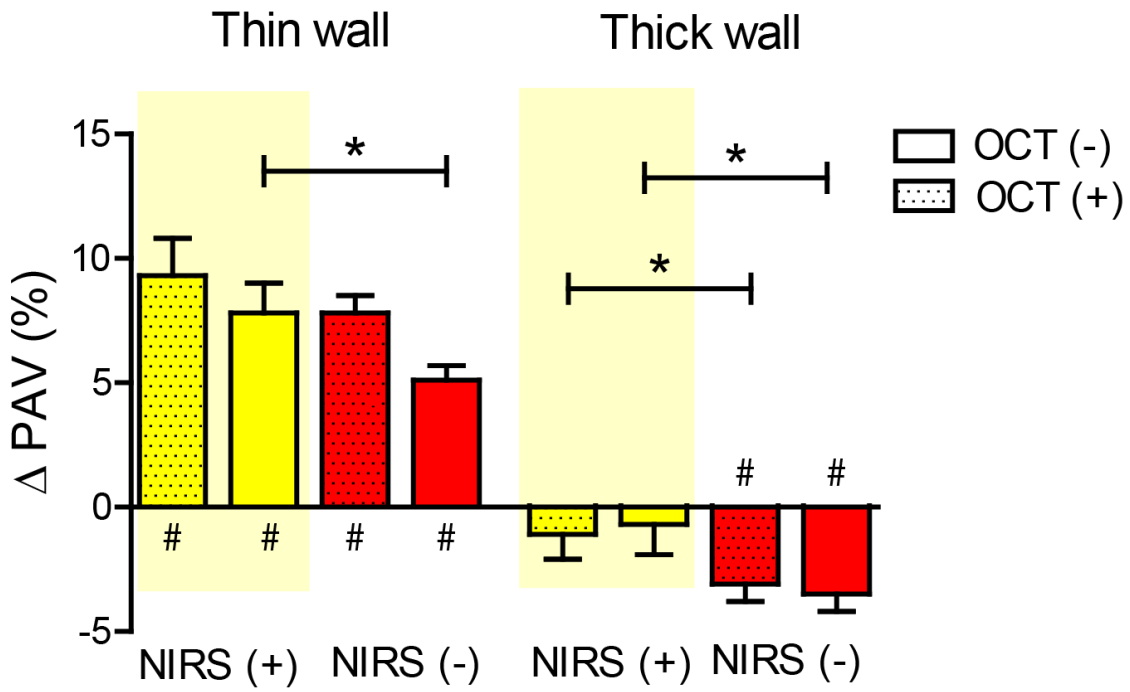

Supplementary Figure 5. Relative plaque area (per sector) progression in thin and thick wall sectors stratified by NIRS and OCT-detected lipid plaque.

Yellow: NIRS positive sectors (NIRS[+]); red: NIRS negative sectors (NIRS[-]); thin, <0.5 mm wall thickness by IVUS; thick; ≥0.5 mm wall thickness by IVUS. OCT(-) sectors that did not demonstrate lipid on OCT; OCT(+): sectors that demonstrated lipid on OCT;

* $p<0.001$, # $p<0.001$.

IVUS: intravascular ultrasound; OCT: optical coherence tomography; NIRS: near-infrared spectroscopy; ΔPAV: Change in relative plaque area